

## Article

# Effects of Ca-Compounds on the Gases Formation Behavior during Molten Salts Thermal Treatment of Bio-Waste

Jing He <sup>1,2</sup>, Chan Zou <sup>1,3</sup>, Xuanzhi Zhou <sup>1</sup>, Yuting Deng <sup>1</sup>, Xi Li <sup>1,3</sup>, Lu Dong <sup>1,3</sup> and Hongyun Hu <sup>1,3,\*</sup>

<sup>1</sup> State Key Laboratory of Coal Combustion, Huazhong University of Science and Technology, Wuhan 430074, China

<sup>2</sup> Department of Architectural Environment and Energy Engineering, Anhui Jianzhu University, Hefei 230009, China

<sup>3</sup> Research Institute, Huazhong University of Science and Technology in Shenzhen, Shenzhen 518000, China

\* Correspondence: hongyunhu@hust.edu.cn; Tel.: +86-27-87542417

**Abstract:** Bio-waste utilization is essential, and pyrolysis is a prominent way for its effective utilization. However, the gradual accumulation of ash compounds in the intermediate products probably affects the thermal conversion characteristics of bio-waste. In the present study, beech wood and disposable chopsticks were selected as bio-waste samples. The effects of typical ash components (Ca-compounds) on volatile formation behavior were investigated during the molten salts thermal treatment of bio-waste. Results demonstrated that about 80% mass of initial bio-waste was gasified into the volatiles at 300 °C. The introduction of Ca-compounds in the molten salts slightly decreased the total yield of gaseous products. More specifically, Ca<sup>2+</sup> could improve the generation of CO<sub>2</sub> and suppress the generation of other gases (CO, H<sub>2</sub>, and CH<sub>4</sub>), and this is accompanied by a reduction in the low heating value (LHV) of the gases. The possible reason is that Ca<sup>2+</sup> might act on the -OH bonds, phenyl C-C bond, methoxy bond and carboxylic acid -COOH bonds of the bio-waste to promote CO<sub>2</sub> release. In contrast, the introduction of CO<sub>3</sub><sup>2-</sup> and OH<sup>-</sup> tended to relieve the inhibition effect of Ca<sup>2+</sup> on the generation of H-containing gases. Meanwhile, the introduction of Ca<sup>2+</sup> can promote the conversion of bio-waste into liquid products as well as increase the saturation level of liquid products. Moreover, as a vital form of carbon storage, CO<sub>2</sub> was found to be abundant in the pyrolysis gases from molten salts thermal treatment of bio-waste, and the concentration of CO<sub>2</sub> was much higher than that of direct-combustion or co-combustion with coal. It's a promising way for bio-waste energy conversion as well as synchronized CO<sub>2</sub> capture by using molten salts thermal treatment, while the introduction of small amounts of Ca-compounds was found to have no significant effect on the change of CO<sub>2</sub> concentration.

**Keywords:** bio-waste; molten salts thermal treatment; gases formation; Ca-compounds; CO<sub>2</sub> capture



**Citation:** He, J.; Zou, C.; Zhou, X.; Deng, Y.; Li, X.; Dong, L.; Hu, H. Effects of Ca-Compounds on the Gases Formation Behavior during Molten Salts Thermal Treatment of Bio-Waste. *Catalysts* **2022**, *12*, 1465. <https://doi.org/10.3390/catal12111465>

Academic Editors: Indra Pulidindi, Pankaj Sharma and Aharon Gedanken

Received: 9 October 2022

Accepted: 14 November 2022

Published: 18 November 2022

**Publisher's Note:** MDPI stays neutral with regard to jurisdictional claims in published maps and institutional affiliations.



**Copyright:** © 2022 by the authors. Licensee MDPI, Basel, Switzerland. This article is an open access article distributed under the terms and conditions of the Creative Commons Attribution (CC BY) license (<https://creativecommons.org/licenses/by/4.0/>).

## 1. Introduction

Energy utilization of bio-waste is one of the prominent ways to mitigate carbon dioxide emissions [1]. However, low energy density and high cost in energy conversion process both restrict the development and application of bio-waste energy technology. Accordingly, many efforts have been made to convert bio-waste into high-valued energy products such as syngas and pyrolysis carbon [2,3]. On the other hand, researchers are committed to reducing the energy consumption cost, to improve the economy of the utilization [4]. During this process, many scholars have attempted to apply solar energy to the bio-waste thermal conversion, aiming at producing economical, high-value gases [5]. Furthermore, in order to solve the stability problems caused by the fluctuation of solar energy [6], molten salts have been used as the reaction medium for heat storage to realize the stable utilization of bio-waste [7]. It is noteworthy that bio-waste contains a certain amount of ash, which has been proved to change the physicochemical properties of molten salts. The accumulation of biomass ash in molten salts will lead to a decrease in the thermal diffusivity and thermal

conductivity as well as an increase in the specific heat capacity of the eutectic system [8]. Therefore, it is necessary to study the influence of ash on bio-waste reaction characteristics during molten salts thermal treatment.

Calcium is one of the most common elements in bio-waste ash, which is absorbed by bio-waste from the natural environment during the growth process [9]. Ca-compounds are the vital components of bio-waste ash, and the content can reach 68.2% in beech bark [10,11]. At the same time, Ca-compounds in the biomass have been confirmed to be involved in the thermal conversion of organic components in bio-waste [12]. In addition, researchers have pointed out that the added Ca-compounds could improve the pyrolysis performance of three-components (cellulose, hemicellulose and lignin), during which the bio-waste pyrolysis could be affected through converting epoxy into aromatic compounds or through cracking into aliphatic derivatives [13,14]. Meanwhile, the presence of Ca also has a certain catalytic effect on the decomposition of pyrolytic oil. Feng et al. explored the effect of Ca on the pyrolysis behavior of rice husk and found that Ca can promote the formation of aldehydes, ketones and acids produced by aromatic ring opening and cracking reactions [15]. Furthermore, Maxim et al. [16] found that Ca played an important role in the reforming of pyrolysis gases. Compared to the conventional pyrolysis process, molten salts thermal treatment could improve the catalytic activity of the reaction and enhance the heat transfer [17]. It is noteworthy that the generation of three-phase (gas-liquid-solid) products would be more intense during molten salts thermal treatment. However, little research has focused on the effects of the bio-waste ash (especially Ca) introduction on the pyrolysis behavior during molten salts thermal treatment.

Many studies have indicated that different Ca-compounds undergo complex thermochemical reactions such as decomposition, carbonation, sulfation, and even electrochemical reaction during bio-waste pyrolysis [18–20]. Therefore, it is worth noting that the role of calcium in the bio-waste thermal treatment process is also related to its species. Yuan et al. evaluated the pyrolysis of bio-waste in the presence of  $\text{CaCO}_3$ , and the results showed that  $\text{CaCO}_3$  can improve the pyrolysis of rice husk [21]. Chen et al. [22] pointed out that the existence of  $\text{Ca(OH)}_2$  increased the biochar yield, and generated larger amounts of phenols and aromatics. In the research of Raymundo et al.,  $\text{Ca(OH)}_2$ ,  $\text{CaO}$  and  $\text{Ca(COOH)}_2$  were further confirmed to promote deoxygenation of bio-oils, and the promotion effect is in the order:  $\text{Ca(OH)}_2$ ,  $\text{CaO}$ , and  $\text{Ca(COOH)}_2$  [23]. In general,  $\text{CaO}$  is an important component of bio-waste ash [10,24,25].  $\text{CaCO}_3$  and  $\text{Ca(OH)}_2$  would be formed by the reaction between  $\text{CaO}$  and a small molecule ( $\text{CO}_2$  and  $\text{H}_2\text{O}$ ) [26]. From the related studies for fuel cells, it was found that the reaction of solid fuel is affected by both cations and anions in molten salts [27–30]. Zeng et al. investigated the pyrolysis of bio-waste using the  $\text{Li}_2\text{CO}_3\text{-Na}_2\text{CO}_3\text{-K}_2\text{CO}_3$  ternary molten salts. Results indicated that alkali metal carbonates were participating in the bio-waste thermal conversion [31]. Various Ca-compounds (like  $\text{CaCO}_3$  and  $\text{Ca(OH)}_2$ ) introduced into the molten salts probably changed the distribution characteristics of anions in the reaction system, which might affect the properties of pyrolysis products in molten salts.

To improve the utilization efficiency of solar energy over a longer period of time, molten nitrates were selected as medium for the storage of solar energy as well as the conversion of bio-waste into high-value gases [32]. In the present study, two typical bio-wastes (beech wood and disposable chopsticks) were selected to comparatively analyze the effects of Ca-compounds on the gas formation behavior during molten salts ( $\text{NaNO}_3\text{-NaNO}_2$ ) thermal treatment. Firstly, considering the dissolution and dispersion characteristics of calcium in the molten salts, the  $\text{Ca(NO}_3)_2$  (only added with  $\text{Ca}^{2+}$ ) was chosen to study the effect of  $\text{Ca}^{2+}$  on the bio-waste pyrolysis characteristics. Subsequently, in order to explore the effect of different Ca-compounds on the pyrolysis characteristics of the two bio-wastes,  $\text{Ca(NO}_3)_2$ ,  $\text{CaCO}_3$ , and  $\text{Ca(OH)}_2$  were added in the molten salts system, respectively. In detail, the gaseous and liquid products were detected using GC and GC-MS to further understand the thermal conversion behavior of the two bio-wastes.

## 2. Results and Discussion

### 2.1. Releasing Characteristics of Gases with the Addition of Different Ca-Compounds

The distribution characteristics of the pyrolysis (including conventional pyrolysis and molten salts thermal treatment) products from beech wood and disposable chopsticks is compared in Figure 1. It's obviously that more bio-waste was converted into pyrolysis gases and liquid products in the case of molten salts thermal treatment, which is consistent with previous studies [8,17]. The mass ratios of volatiles from the two bio-wastes ranged from 79.4% to 89.3% during the molten salts thermal treatment, while the volatile yield was 18.3% to 20.5% in conventional pyrolysis. It suggests that molten salts probably had a catalytic effect on the release of volatiles during bio-waste pyrolysis, regardless of the type of the bio-waste. After the addition of various Ca-compounds, the distribution characteristics of the volatiles (including gaseous and liquid products) were changed, to a certain extent, ranging from 79.8% to 85.6% for beech wood and from 79.4% to 87.5% for disposable chopsticks. Moreover, the gas yield ranged from 54.6% to 62.3% for beech wood and from 55.4% to 63.3% for disposable chopsticks.

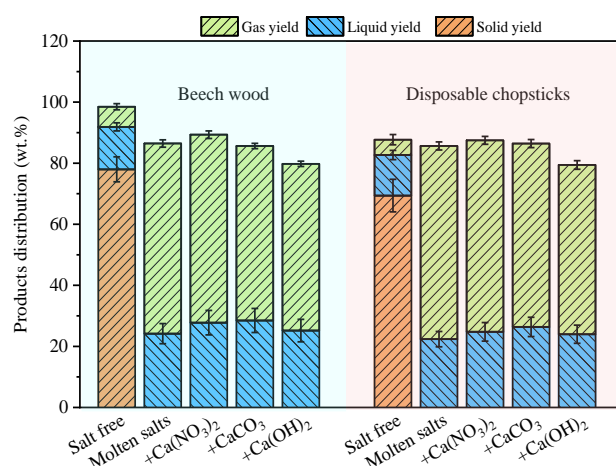


**Figure 1.** Products distribution in salt free/molten salts pyrolysis of the two bio-wastes.

In order to further explore the effect of  $\text{Ca}^{2+}$  on bio-waste pyrolysis characteristics, different contents of  $\text{Ca}(\text{NO}_3)_2$  were selected to study the gas generation characteristics during molten salts thermal treatment. As shown in Figure 2, compared with the conventional pyrolysis (salt-free), more gaseous products were generated from the selected bio-waste in the molten salts pyrolysis. It is supposed that the catalysis of ions in molten salts greatly reduced the reaction activation energy during bio-waste pyrolysis [17]. In addition, the gas yield was reduced with the addition of  $\text{Ca}(\text{NO}_3)_2$ , and the inhibition effect was more obvious with an increase in  $\text{Ca}(\text{NO}_3)_2$  content. On the one hand, the introduction of  $\text{Ca}^{2+}$  may change the physicochemical properties of molten salts [28]. On other hand,  $\text{Ca}^{2+}$  could promote the synthesis of small molecules, which then decreased the pyrolysis gas yield. In conventional pyrolysis (salt-free) process, the gaseous product is only  $\text{CO}_2$  at 300 °C, which is mostly produced from the decomposition of low- thermal-stability components in the bio-waste [33]. From Figure 3, adding 10 g  $\text{Ca}(\text{NO}_3)_2$  could promote the  $\text{CO}_2$  yield, while excess  $\text{Ca}(\text{NO}_3)_2$  might suppress the formation of  $\text{CO}_2$ . It is suggested that  $\text{Ca}^{2+}$  promotes the release of  $\text{CO}_2$  by breaking the-OH bond, phenyl C-C, and methoxy and carboxylic acid-COOH bonds, which attach to the end of the bio-waste molecular structure [34]. However, excess  $\text{Ca}^{2+}$  may inhibit the transfer of  $\text{NO}_3^-$  to  $\text{NO}_2^-$ , which has been proved to play an important role for the bio-waste pyrolysis [32]. Thus, the excess  $\text{Ca}(\text{NO}_3)_2$  further reduces the gases yield, and will decrease the  $\text{CO}_2$  concentration in pyrolysis gases.

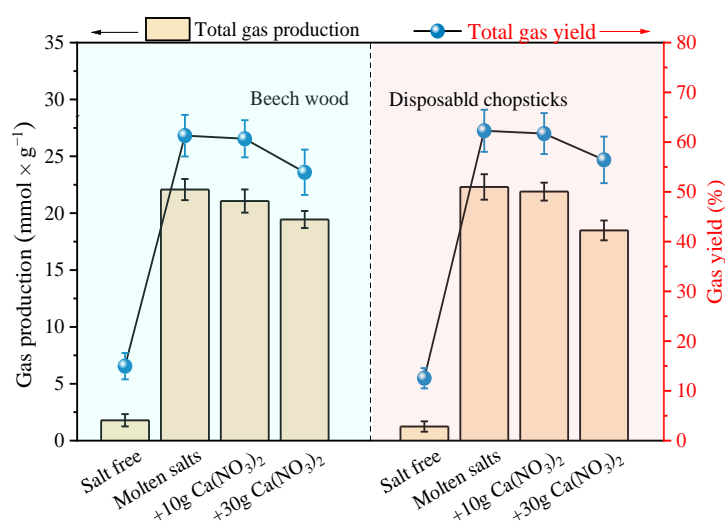


**Figure 2.** The generation properties of pyrolysis gases under different conditions.

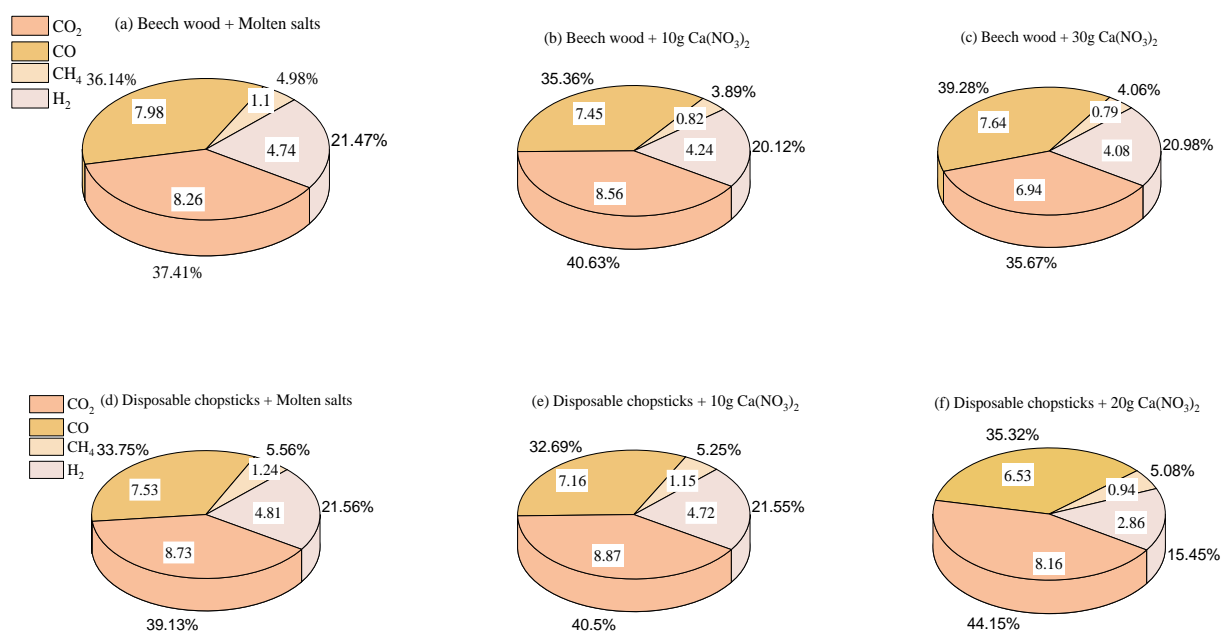


**Figure 3.** Gas distribution characteristics of the bio-wastes during NaNO<sub>3</sub>-NaNO<sub>2</sub> adding Ca(NO<sub>3</sub>)<sub>2</sub> (a–c) Beech wood (d–f) Disposable chopsticks.

The gas yield of the examined two bio-wastes with the addition of different Ca-compounds are shown in Figure 4a. The gas yield all decreased after the addition of Ca-compounds (Ca(NO<sub>3</sub>)<sub>2</sub>, CaCO<sub>3</sub>, and Ca(OH)<sub>2</sub>), which was consistent with previous work [23,35]. Among those Ca-compounds, Ca(OH)<sub>2</sub> seems to have had the strongest inhibitory effect on the pyrolysis gases generation, which decreased by 12.33% for beech wood and 12.37% for disposable chopsticks. It has been pointed out that OH<sup>-</sup> could inhibit decarbonylation (C-O) and decarboxylation (C-O-C) in hemicellulose [36]. Another reason is that CO<sub>2</sub> can be easily captured by Ca(OH)<sub>2</sub> to form CaCO<sub>3</sub>(s). Moreover, the distribution of different gaseous products are presented in Figure 4b. Compared with the NaNO<sub>3</sub>-NaNO<sub>2</sub> system, the addition of Ca-compounds hardly changed the types of gaseous products during the pyrolysis process, while it did affect the yield of each gas.

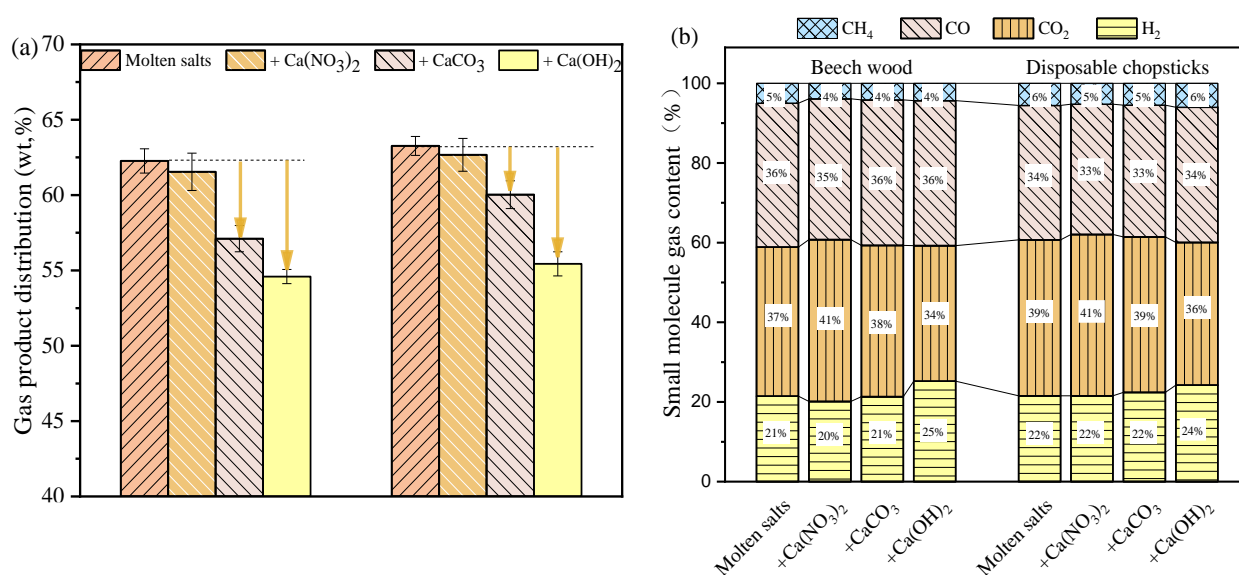


**Figure 4.** The distribution characteristics of gaseous products in molten salts pyrolysis. (a) Gas yield, (b) distributions of small molecules.

## 2.2. Effects of Ca-Compounds on Combustible Gases Release in Molten Salts

The change ratios of different small molecule gases (H<sub>2</sub>, CO<sub>2</sub>, CO, and CH<sub>4</sub>) produced during the thermal conversion of beech wood and disposable chopsticks are shown in Figure 5. Compared with NaNO<sub>3</sub>-NaNO<sub>2</sub> salt, the conversion ratios of combustible gases (H<sub>2</sub>, CO, and CH<sub>4</sub>) decreased with the addition of Ca(NO<sub>3</sub>)<sub>2</sub>. It should be pointed out that the only distinction between the two molten salts is the existence of Ca<sup>2+</sup>, which could inhibit the decomposition of components, resulting in the yield decrease of gaseous products during the pyrolysis process [37]. Notice that CO<sub>2</sub> increased by 3.63% and 1.60%, respectively, after adding Ca(NO<sub>3</sub>)<sub>2</sub> in the thermal conversion process of beech wood and disposable chopsticks. Ca<sup>2+</sup> will attach to the pyran ring of the bio-waste, and the ion effect will make it prone to ring-opening decarbonylation (C=O) at C1~C2, C1~O5, C3~C4, and C5~O5. Thus, more CO<sub>2</sub> could be formed through the decarbonylation (C=O) reaction [38,39]. It indicates that the introduction of carbon dioxide could dilute the calorific value of combustible gas in the mixture.

Compared to molten salts with Ca(NO<sub>3</sub>)<sub>2</sub>, the introduction of CaCO<sub>3</sub> and Ca(OH)<sub>2</sub> provide OH<sup>-</sup> and CO<sub>3</sub><sup>2-</sup>. From Figure 5, taking the NaNO<sub>3</sub>-NaNO<sub>2</sub> as the control, the ratios of total H-containing gases (H<sub>2</sub> and CH<sub>4</sub>) were changed by -15.27%, -13.98% and 0.86% in those three molten salts systems for beech wood, and -3.70%, -2.33% and 1.78% for disposable chopsticks. It was concluded that OH<sup>-</sup> and CO<sub>3</sub><sup>2-</sup> can relieve the negative effect of Ca<sup>2+</sup> on the generation of H-containing gases. The reason is that Ca(OH)<sub>2</sub> can provide more dissociative OH<sup>-</sup>, which can reduce the energy of C-H bond-breaking in cellulose and promote H-containing gas production [40,41]. Moreover, CO<sub>3</sub><sup>2-</sup> can significantly promote the cracking and deformation of C=C and C-H groups, and thus increase the formation of H-containing gases [42].

As shown in Figure 6, compared with conventional pyrolysis, more bio-waste is converted into the liquid volatile at 300 °C. The main reason is that NO<sub>2</sub><sup>-</sup> in molten salts could play a prominent catalytic role, and the presence of Na<sup>+</sup> can lower the pyrolysis temperature. Meanwhile, NO<sub>2</sub><sup>-</sup> can participate in the reaction to form more volatiles, leading to a higher liquid yield [32]. Moreover, the addition of Ca-compounds promotes the yield of liquid products, which is in agreement with the previous work [13]. The reason is that Ca-compounds may enhance the process of dehydroxyl, which is beneficial at forming liquid volatiles during the pyrolysis process. Furthermore, the promotion degree of different Ca-compound is in the order: CaCO<sub>3</sub> > Ca(NO<sub>3</sub>)<sub>2</sub> > Ca(OH)<sub>2</sub>. Therefore,

the introduction of Ca-compounds can promote the formation of macromolecular liquid volatiles from bio-waste and reduce the yield of gas products.

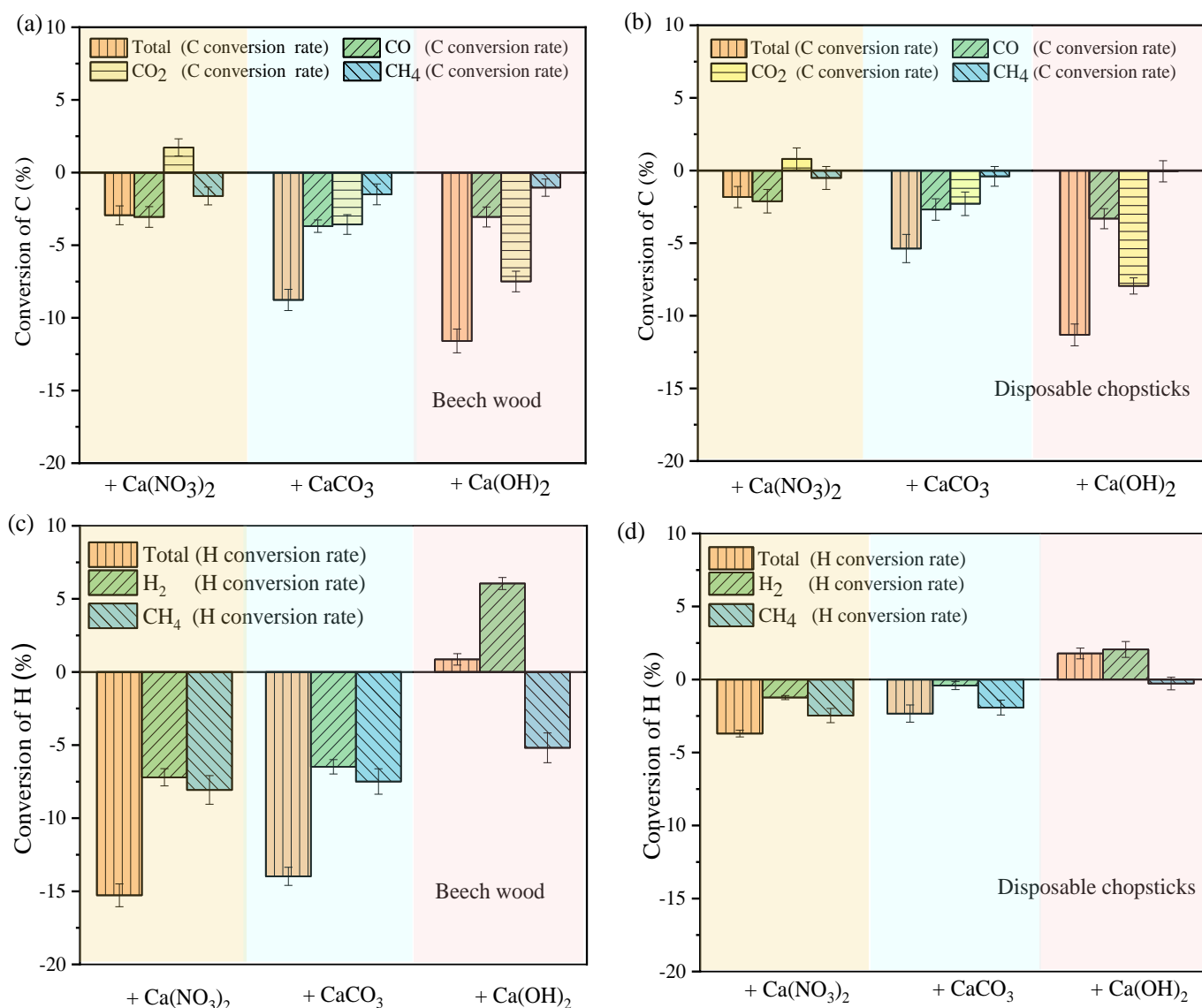


**Figure 5.** Effects of  $\text{Ca}(\text{NO}_3)_2/\text{CaCO}_3/\text{Ca}(\text{OH})_2$  on the conversion of C or H of the small molecule gas. (a) C conversion rate of beech wood, (b) C conversion rate of disposable chopsticks, (c) H conversion rate of beech wood, (d) H conversion rate of disposable chopsticks.

In order to clearly explain the release characteristics of small molecule gas, the major organic composition of liquid products from the two bio-wastes were analyzed, as presented in Figure 7. CG-MS was used to test the composition and relative content of liquid products, and the major organic composition matter by functional group classification statistics. In this experiment, the liquid products were mainly divided into furan, aldehyde ketone, phenol, aromatic hydrocarbon and nitrogen-containing compounds. For the beech wood and disposable chopsticks, the introduction of  $\text{Ca}(\text{NO}_3)_2$ ,  $\text{CaCO}_3$ , and  $\text{Ca}(\text{OH})_2$  inhibited the formation of furan and phenols, while it enhanced the formation of ketones/aldehydes. Ca-compounds will reduce the formation of oxygen-containing compounds (like phenols), because Ca-compounds can enhance the deoxygenation reaction of bio-waste pyrolysis [43,44]. The catalytic action of Ca can promote the formation of ketones/aldehydes by ring opening and cracking of aromatic rings [45,46].

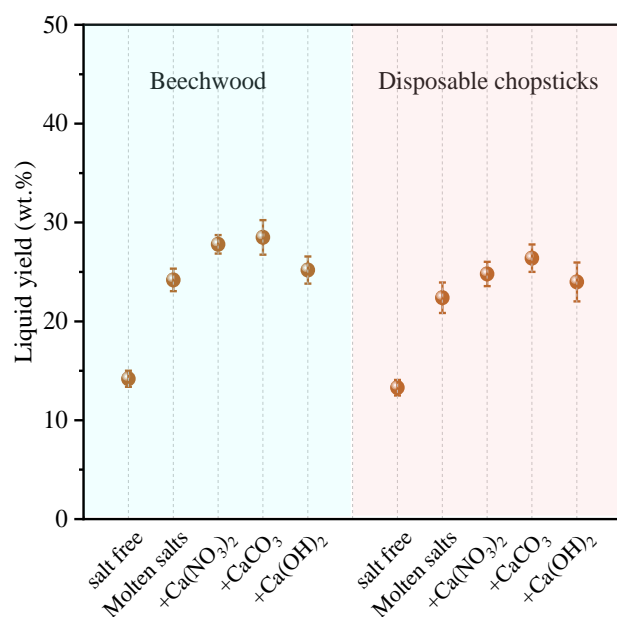


**Figure 6.** Liquid yield of thermal conversion in molten salts with different Ca-compounds.

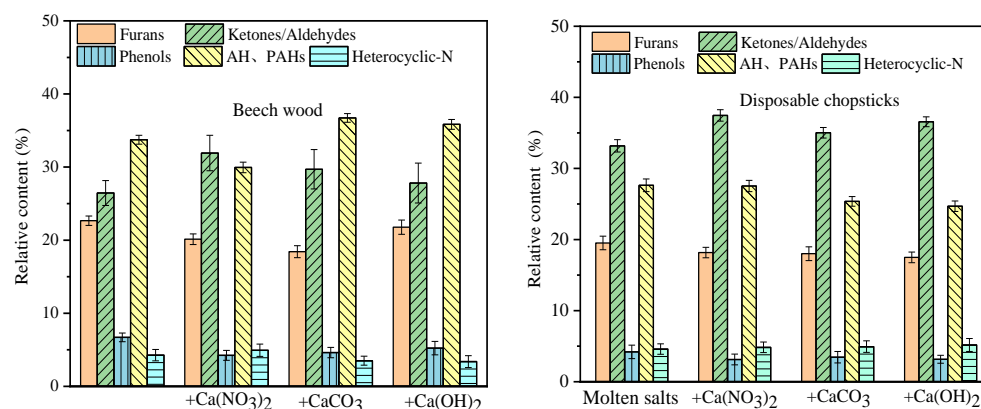


**Figure 7.** Liquid products of thermal conversion in molten salts.

Moreover, in order to explore the effect of Ca-compounds on the saturation level of liquid products, the ratios of C/H in liquid products in different molten salts systems were calculated, as shown in Figure 8. The curves of the C/H ratios in liquid products were calculated after removing the O atom for those molten salts systems. O atoms in liquid products could be removed according to the following routes. First, The -OH was removed due to the internal dehydration reaction. Secondly, CO<sub>2</sub> was produced by the cleavage/reforming of carboxyl (O-C=O) and carbonyl (C-O-C) groups. Thirdly, CO was mainly generated by cleavage of lignin units and diaryl ether bonds and ether bridges [47,48]. In general, the saturation level of the liquid phase product was inversely proportional to the C/H ratio in liquid products, and the change of C/H ratio in liquid products was used to characterize the changing trend of the saturation level of the liquid product. A higher C/H ratio in liquid products corresponds to a lower saturation level. From Figure 8, it could be seen that the C/H ratio in liquid products corresponding to the highest content decreased with the addition of Ca-compounds, which indicates that Ca<sup>2+</sup> can promote the saturation level of liquid products. As mentioned above, compared to NaNO<sub>3</sub>-NaNO<sub>2</sub> system, the addition of Ca-compounds will decrease the yield of H-containing gases, and in turn promote the saturation level of liquid products. In addition, the degree of decrease for the C/H ratio in liquid products is as follows: Ca(NO<sub>3</sub>)<sub>2</sub> > CaCO<sub>3</sub> > Ca(OH)<sub>2</sub>. Compared with Ca(NO<sub>3</sub>)<sub>2</sub>, CO<sub>3</sub><sup>2-</sup> and OH<sup>-</sup> were introduced in NaNO<sub>3</sub>-NaNO<sub>2</sub> salt for CaCO<sub>3</sub> and Ca(OH)<sub>2</sub>, which

suggested that anions may relieve the inhibition effect of  $\text{Ca}^{2+}$  on the saturation level of bio-waste pyrolysis products.

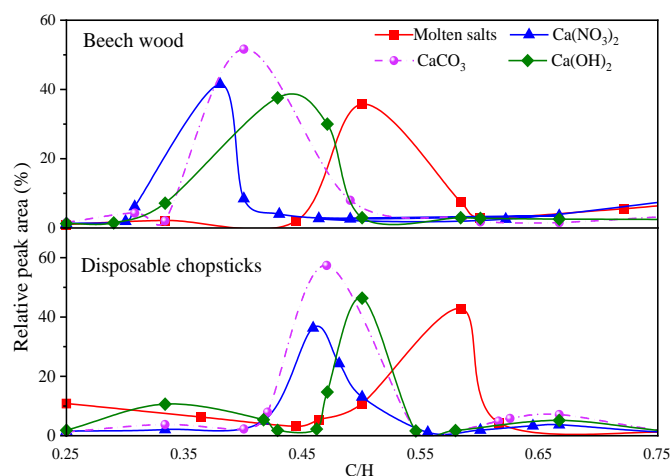


**Figure 8.** Effects of  $\text{Ca}(\text{NO}_3)_2/\text{CaCO}_3/\text{Ca}(\text{OH})_2$  on the saturation level of the liquid products.

### 2.3. Application and Discussion

The combustible gases can be used in many ways, such as power generation, heating systems, and so on. In addition, the high concentration of  $\text{CO}_2$  is a benefit for its recycling, which is an effective way to reduce carbon emissions. The LHVs of bio-waste pyrolysis gases were calculated according to their yield and composition, and the results are listed in Figure 9. The LHVs of pyrolysis gases are marked with black dots, and red dots represent the LHVs without  $\text{CO}_2$ . From Figure 9, the LHVs obviously varied with the addition of different calcium mixtures, while the LHVs of pyrolysis gases without  $\text{CO}_2$  changed little. The reason is that the Ca-compounds have the greatest impact on  $\text{CO}_2$  generation compared with other pyrolysis gases. In addition, for the pyrolysis gases of beech wood and disposable chopsticks, the LHVs ( $13.83 \text{ MJ}/\text{Nm}^3$  and  $14.08 \text{ MJ}/\text{Nm}^3$ ) without  $\text{CO}_2$  were significantly higher than that ( $8.66 \text{ MJ}/\text{Nm}^3$  and  $8.57 \text{ MJ}/\text{Nm}^3$ ) with  $\text{CO}_2$ .

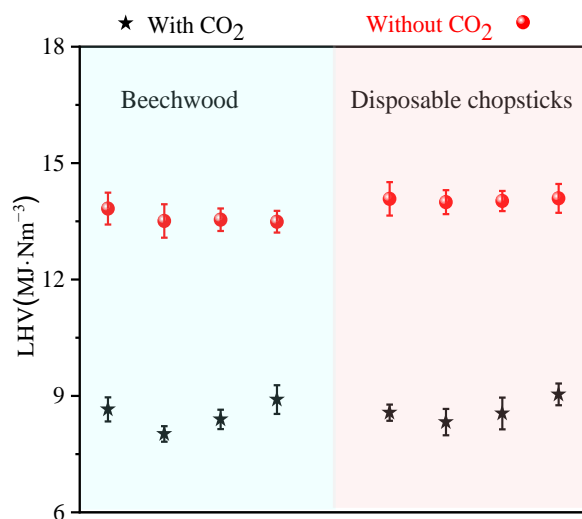


**Figure 9.** Effects of  $\text{Ca}(\text{NO}_3)_2/\text{CaCO}_3/\text{Ca}(\text{OH})_2$  on LHVs of small molecule gas: with/without  $\text{CO}_2$ .

Combined with Figures 4b and 9, the LHVs of pyrolysis gases with the addition of  $\text{Ca}(\text{NO}_3)_2$  and  $\text{CaCO}_3$  were lower than that in  $\text{NaNO}_3\text{-NaNO}_2$  salt. The main reason is that the addition of the two Ca compounds would increase the proportion of  $\text{CO}_2$  in the pyrolysis gases. In addition, it was found that the LHVs of pyrolysis gases with the



addition of  $\text{Ca}(\text{OH})_2$  were the highest for those two bio-wastes in Figure 9. As mentioned in Section 2.2, although the total gas yield reduced in the presence of  $\text{OH}^-$ , the proportion of the combustible gas increased in this circumstance.

The capture and utilization of  $\text{CO}_2$  can not only effectively reduce the pressure of greenhouse gas emissions, but also produce huge economic benefits [49]. In Figure 10, the five-pointed stars and dots represent the  $\text{CO}_2$  concentration after pyrolysis gas (including and excluding  $\text{CO}_2$ ) combustion. As to the pyrolysis gases in different molten salts systems, the  $\text{CO}_2$  concentrations was 23.6%, 25.2%, 24.1% and 22.6% for beech wood, respectively, and 24.1%, 24.5%, 23.8% and 22.5% for disposable chopsticks, respectively. From the results, the  $\text{CO}_2$  concentration after pyrolysis gas combustion was much higher than that for bio-waste direct-combustion and for coal-fired power plants. As for the bio-wastes studied in the paper, the introduction of Ca-compounds can increase the  $\text{CO}_2$  concentration after pyrolysis gas combustion, which is a benefit for the  $\text{CO}_2$  separation and capture [50].

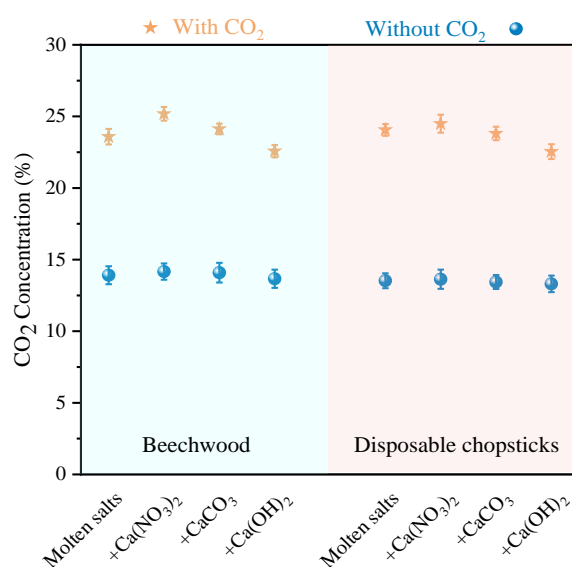


**Figure 10.**  $\text{CO}_2$  concentration after combustion: with/without  $\text{CO}_2$  before combustion.

Figure 11 shows that the main negative carbon reactions during molten salt pyrolysis, and  $\text{CO}_2$  cycling would be accompanied by energy conversion during this process. In detail, for the energy conversion, solar energy is used for photosynthesis of plants and for heating low-temperature molten salts in this work. A large amount of combustible gas would be generated from waste bio-waste after molten salts thermal conversion. In addition, for  $\text{CO}_2$  cycling, the combustible gas will generate  $\text{CO}_2$  again, and then the  $\text{CO}_2$  could be absorbed and stored by a capture system.

In particularly, ash matter would remain and change the physicochemical properties of molten salts during the thermal treatment process. In this paper,  $\text{Ca}(\text{NO}_3)_2/\text{CaCO}_3/\text{Ca}(\text{OH})_2$  were simulated as the main impurities to explore their effect on the pyrolysis characteristics of bio-waste in molten salts. Summarily,  $\text{Ca}^{2+}$  can promote the  $\text{CO}_2$  concentration of pyrolysis gases, while the accompanying anions ( $\text{CO}_3^{2-}$ ,  $\text{OH}^-$ ) weaken this promotional effect by increasing the concentration of H-containing gases. Overall, bio-waste thermal conversion could be a potential carbon capture method.

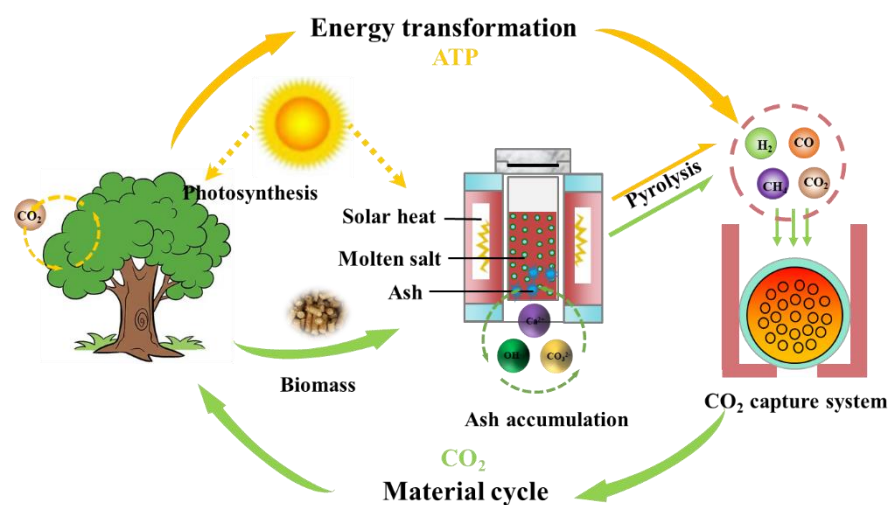


**Figure 11.** Main negative carbon reaction pathways of bio-waste pyrolysis in molten salts.

### 3. Materials and Methods

#### 3.1. Materials

Two typical kinds of bio-waste, beech wood and disposable chopsticks were used in the present study. Beech wood is a common furniture material, which has the characteristics of stable wood property; hard material, impact resistance, and difficulty to deform. In addition, disposable chopsticks were selected to conduct pyrolysis experiments due to its huge abundance in China. Strips or tablets (1–2 cm) of feedstocks were dried at 105 °C for 24 h in an oven before the experiments. Analytical grade reactants,  $\text{NaNO}_3$ - $\text{NaNO}_2$  (SCR Co., Ltd., Shanghai, China) molten salts was physically mixed with a weight ratio of 56.3–43.7%. The three Ca-compounds,  $\text{Ca}(\text{NO}_3)_2$ - $\text{CaCO}_3$ - $\text{Ca}(\text{OH})_2$  (SCR Co., Ltd., Shanghai, China), were obtained with an analytical grade. It should be noted that  $\text{Ca}(\text{NO}_3)_2 \cdot 4\text{H}_2\text{O}$  was used to substitute for  $\text{Ca}(\text{NO}_3)_2$ .

The proximate/ultimate analysis results and three-components of beech wood and disposable chopsticks are listed in Table 1.

**Table 1.** Proximate and ultimate analysis on dry basis and three-components of the samples.

Samples	Proximate Analysis (wt%)			Ultimate Analysis (wt%)					Cellulose	Hemicellulose	Lignin
	V <sub>d</sub>	FC <sub>d</sub>	A <sub>d</sub>	C	H	O <sup>a</sup>	N	S			
Beech wood	85.4	13.2	1.4	45.2	5.7	49.1	- <sup>b</sup>	-	47.3	15.2	28.4
Disposable chopsticks	80.0	18.7	1.3	45.3	5.6	48.7	0.3	0.1	32.9	29.4	19.2

<sup>a</sup> Calculated by difference. <sup>b</sup> Not detected.

#### 3.2. Experimental Methods

In this experiment, 300 g of the mixed salt was added to the reactor (shown in Figure 12) and heated to 300 °C, and then the temperature was kept for at least 3 h to form a homogeneous liquid phase before experiments. In order to study the effect of  $\text{Ca}^{2+}$ , 10 g or 30 g of  $\text{Ca}(\text{NO}_3)_2$  were added to the molten salts system. In addition, to explore the effect of different Ca-compounds on the pyrolysis behavior of the bio-wastes, 10 g of  $\text{Ca}(\text{NO}_3)_2$ ,  $\text{CaCO}_3$ , and  $\text{Ca}(\text{OH})_2$  were introduced into the molten salts, respectively. Considering the consumption of molten salts and the accumulation of impurities during the experiment, the number of experiments in each reactor was less than 12 groups. This ensures that the experimental results cannot be affected by the attenuation of the molten salts performance. In the experiments, about 1 g of the sample was added to the metal pocket placed above the molten salts, and nitrogen gas was constantly input to the reactor at 700 mL/min. Then, the nitrogen gas flowed for 3 min to evacuate the air in the reactor and pipeline. After that, the sample was put into the molten salts for 10 min thermal treatment. The U-shaped tubes

were bathed in the liquid nitrogen to collect the liquid products. Meanwhile, the gaseous products were collected in a gasbag for subsequent experimental tests. After the pyrolysis process, the metal mesh pocket was lifted by connected rods from the molten salts to the upper part of the reactor, then cooled by nitrogen, and taken out at last.

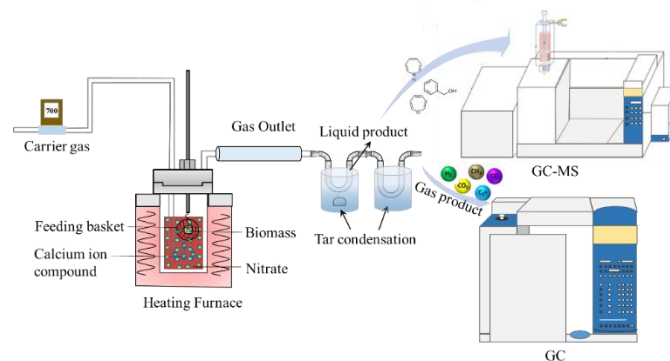


**Figure 12.** Schematic diagram of the molten salts pyrolysis reactor.

### 3.3. Analytical Methods

An element analyzer (Vario Micro cube, Elementar, Langensfeld, Germany) was employed to determine the carbon, hydrogen nitrogen and sulfur content. The proximate analysis was measured according to GB/T28731-2012. The LHV of gaseous products was calculated through Equation (1):

$$\text{LHV (MJ/Nm}^3) = 12.6 \times y_{\text{CO}} + 10.8 \times y_{\text{H}_2} + 35.8 \times y_{\text{CH}_4} \quad (1)$$

where,  $y_{\text{CO}}$ ,  $y_{\text{H}_2}$  and  $y_{\text{CH}_4}$  are the volume fractions (vol%) of carbon monoxide, hydrogen and hydrocarbons in the gaseous products respectively [51].

The water content of liquid products was examined with a Volumetric KF Titrator (V10S, Mettler Toledo, Greifensee, Switzerland). The chemical composition of tar was determined with using GC-MS (Agilent, 7890A/5975C, Santa Clara, CA, USA) with a capillary column (Agilent: HP-5MD, 19091s-433; 30 m  $\times$  0.25 mm i.d.  $\times$  0.25  $\mu\text{m}$  d.f.). The injection volume of each sample was 1  $\mu\text{L}$ , and the split ratio was 1:1. The gaseous products were analyzed with a GC (Agilent 7890B, USA). The compounds were identified using a National Institute of Standards and Technology library (NIST14.L).

## 4. Conclusions

In the present work, two bio-wastes (beech wood-disposable chopsticks) were selected to reveal the effects of Ca-compounds ( $\text{Ca}(\text{NO}_3)_2$ ,  $\text{CaCO}_3$ ,  $\text{Ca}(\text{OH})_2$ ) on the gas formation characteristics in a nitrates ( $\text{NaNO}_3$ - $\text{NaNO}_2$ ) system. The main conclusions of this study are as following: the mass ratios of the volatiles from the two bio-wastes were much higher (86.4% and 85.6%) during molten salts thermal treatment than that in conventional pyrolysis (20.5% and 18.3%) at 300  $^\circ\text{C}$ . The main reason is that the ions in molten salts greatly reduced the reaction activation energy during the bio-waste pyrolysis process. As for the gaseous products, the addition of Ca-compounds in molten salts would slightly reduce the gas yield. Moreover,  $\text{Ca}(\text{OH})_2$  seems to have the strongest inhibitory effect on the pyrolysis gas generation, decreasing the gas production by 12.33% for beech wood and 12.37% for disposable chopsticks. From the perspective of ions,  $\text{Ca}^{2+}$  can promote the production of  $\text{CO}_2$ , while the release of other gases ( $\text{CO}$ ,  $\text{H}_2$  and  $\text{CH}_4$ ) will be inhibited. At the same time, the  $\text{OH}^-$  and  $\text{CO}_3^{2-}$  could relieve the effect of  $\text{Ca}^{2+}$  on gas formation. For the liquid products, the introduction of  $\text{Ca}^{2+}$  increases the saturation level of liquid products as well as increases the liquid yield. In particular, the addition of  $\text{CaCO}_3$  contributed to an increase in liquid yield from 24.2% to 28.5% for beech wood and from 22.4% to 26.7% for disposable chopsticks. The addition of Ca-compounds in molten salts could increase the  $\text{CO}_2$  concentration after the combustion of pyrolytic gases, which would benefit  $\text{CO}_2$

separation and capture. Meanwhile, it is suggested that molten salts thermal treatment is a promising carbon negative technology to achieve carbon neutrality.

**Author Contributions:** Investigation, writing original Draft, writing review & editing, J.H.; Data Curation, formal analysis, C.Z.; Resources, formal analysis, X.Z.; Writing Review & Editing Y.D.; Methodology, supervision X.L.; Supervision, methodology, resources, funding acquisition, writing review & editing, L.D.; Conceptualization, resources, supervision, writing review & editing. H.H. All authors have read and agreed to the published version of the manuscript.

**Funding:** Shenzhen Science and Technology Innovation Committee (JCYJ20210324115606017), The Key Research and Development Plan of Hubei Province (2022BCA085), and Anhui University Natural Science Research Project (KJ2021JD11).

**Data Availability Statement:** Data are available upon request.

**Acknowledgments:** The authors gratefully acknowledge the assistance of the Analytic and Testing Center of Huazhong University of Science and Technology for the experimental measurements.

**Conflicts of Interest:** The authors declare no conflict of interest.

## References

1. Perumal, S.; Kishore, S.C.; Atchudan, R.; Sundramoorthy, A.K.; Alagan, M.; Lee, Y.R. Sustainable Synthesis of N/S-Doped Porous Carbon from Waste-Biomass as Electroactive Material for Energy Harvesting. *Catalysts* **2022**, *12*, 436. [\[CrossRef\]](#)
2. Xu, T.; Xu, J.; Wu, Y. Hydrogen-Rich Gas Production from Two-Stage Catalytic Pyrolysis of Pine Sawdust with Calcined Dolomite. *Catalysts* **2022**, *12*, 131. [\[CrossRef\]](#)
3. Feng, D.D.; Zhao, Y.J.; Zhang, Y.; Xu, H.H.; Zhang, L.Y.; Sun, S.Z. Catalytic mechanism of ion-exchanging alkali and alkaline earth metallic species on biochar reactivity during CO<sub>2</sub>/H<sub>2</sub>O gasification. *Fuel* **2018**, *212*, 523–532. [\[CrossRef\]](#)
4. Knight, P.; Biewald, B.; Takahashi, K. The cost of energy efficiency programs: Estimates from utility-reported datasets. *Energy* **2022**, *239*, 122448. [\[CrossRef\]](#)
5. Xu, T.; Zheng, X.R.; Xu, J.; Wu, Y.P. Hydrogen-Rich Gas Production from Two-Stage Catalytic Pyrolysis of Pine Sawdust with Nano-NiO/Al<sub>2</sub>O<sub>3</sub> Catalyst. *Catalysts* **2022**, *12*, 256. [\[CrossRef\]](#)
6. Wunn, H.N.; Motoda, S.; Morita, M. Fabrication and Characterization of a Marine Wet Solar Cell with Titanium Dioxide and Copper Oxides Electrodes. *Catalysts* **2022**, *12*, 99. [\[CrossRef\]](#)
7. Zeng, K.; Li, J.; Xie, Y.P.; Yang, H.P.; Yang, X.Y.; Zhong, D.; Zhen, W.X.; Flamant, G.; Chen, H. Molten salt pyrolysis of biomass: The mechanism of volatile reforming and pyrolysis. *Energy* **2020**, *213*, 118801. [\[CrossRef\]](#)
8. Shen, J.H.; Hu, H.Y.; Xu, M.; Liu, H.; Xu, K.; Zhang, X.J.; Yao, H.; Naruse, I. Interactions between molten salts and ash components during Zhundong coal gasification in eutectic carbonates. *Fuel* **2017**, *207*, 365–372. [\[CrossRef\]](#)
9. Nzihou, A.; Stanmore, B.; Lyczko, N.; Minh, D.P. The catalytic effect of inherent and adsorbed metals on the fast/flash pyrolysis of biomass: A review. *Energy* **2019**, *170*, 326–337. [\[CrossRef\]](#)
10. Vassilev, S.V.; Vassileva, C.G.; Song, Y.-C.; Li, W.-Y.; Feng, J. Ash contents and ash-forming elements of biomass and their significance for solid biofuel combustion. *Fuel* **2017**, *208*, 377–409. [\[CrossRef\]](#)
11. Richard, W.B. Fireside slagging, fouling, and high-temperature corrosion of heat-transfer surface due to impurities in steam-raising fuels. *Prog. Energy Combust.* **1996**, *29*, 120.
12. Jiang, L.; Hu, S.; Wang, Y.; Su, S.; Sun, L.S.; Xu, B.Y.; He, L.; Xiang, J. Catalytic effects of inherent alkali and alkaline earth metallic species on steam gasification of biomass. *Int. J. Hydrogen Energy* **2015**, *40*, 15460–15469. [\[CrossRef\]](#)
13. Cui, Y.; Wang, W.L.; Chang, J.M. Study on the Product Characteristics of Pyrolysis Lignin with Calcium Salt Additives. *Materials* **2019**, *12*, 1609. [\[CrossRef\]](#) [\[PubMed\]](#)
14. Li, F.Y.; Gui, X.Y.; Ji, W.C.; Zhou, C.H. Effect of calcium dihydrogen phosphate addition on carbon retention and stability of biochars derived from cellulose, hemicellulose, and lignin. *Chemosphere* **2020**, *251*, 126335. [\[CrossRef\]](#) [\[PubMed\]](#)
15. Feng, D.D.; Zhang, Y.; Zhao, Y.J.; Sun, S.Z. Catalytic effects of ion-exchangeable K<sup>+</sup> and Ca<sup>2+</sup> on rice husk pyrolysis behavior and its gas–liquid–solid product properties. *Energy* **2018**, *152*, 166–177. [\[CrossRef\]](#)
16. Stonor, M.R.; Ouassil, N.; Chen, J.G.; Park, A.-H.A. Investigation of the role of Ca(OH)<sub>2</sub> in the catalytic Alkaline Thermal Treatment of cellulose to produce H<sub>2</sub> with integrated carbon capture. *J. Energy Chem.* **2017**, *26*, 984–1000. [\[CrossRef\]](#)
17. Yang, Y.; Hu, H.; Yang, F.; Tang, H.; Liu, H.; Yi, B.; Li, X.; Yao, H. Thermochemical conversion of lignocellulosic bio-waste via fast pyrolysis in molten salts. *Fuel* **2020**, *278*, 118228. [\[CrossRef\]](#)
18. Tang, G.; Gu, J.; Huang, Z.; Yuan, H.; Chen, Y. Cellulose gasification with Ca–Fe oxygen carrier in chemical-looping process. *Energy* **2021**, *239*, 122204. [\[CrossRef\]](#)
19. Ozgurluk, Y. Investigation of oxidation and hot corrosion behavior of molybdenum coatings produced by high-velocity oxy-fuel coating method. *Surf. Coat. Technol.* **2022**, *444*, 128641. [\[CrossRef\]](#)

20. Odabas, O.; Ozgurluk, Y.; Ozkan, D.; Binal, G.; Calis, I.; Karaoglanli, A.C. Investigation of vermiculite infiltration effect on microstructural properties of thermal barrier coatings (TBCs) produced by electron beam physical vapor deposition method (EB-PVD). *Surf. Coat. Technol.* **2022**, *443*, 128645. [[CrossRef](#)]
21. Yuan, R.; Yu, S.; Shen, Y. Pyrolysis and combustion kinetics of lignocellulosic biomass pellets with calcium-rich wastes from agro-forestry residues. *Waste Manag.* **2019**, *87*, 86–96. [[CrossRef](#)] [[PubMed](#)]
22. Chen, W.; Li, K.; Chen, Z.; Xia, M.; Chen, Y.; Yang, H.; Chen, X.; Chen, H. A new insight into chemical reactions between biomass and alkaline additives during pyrolysis process. *Proc. Combust. Inst.* **2020**, *38*, 3881–3890. [[CrossRef](#)]
23. Raymundo, L.M.; Mullen, C.A.; Boateng, A.A.; DeSisto, W.J.; Trierweiler, J.O. Production of Partially Deoxygenated Pyrolysis Oil from Switchgrass via  $\text{Ca}(\text{OH})_2$ , CaO, and  $\text{Ca}(\text{COOH})_2$  Cofeeding. *Energy Fuel*. **2020**, *34*, 12616–12625. [[CrossRef](#)]
24. Vassilev, S.V.; Vassileva, C.G.; Baxter, D. Trace element concentrations and associations in some biomass ashes. *Fuel* **2014**, *129*, 292–313. [[CrossRef](#)]
25. Dutta, S.; Zhang, Q.; Cao, Y.; Wu, C.; Moustakas, K.; Zhang, S.; Wong, K.; Tsang, D.C. Catalytic valorisation of various paper wastes into levulinic acid, hydroxymethylfurfural, and furfural: Influence of feedstock properties and ferric chloride. *Bioresour. Technol.* **2022**, *357*, 127376. [[CrossRef](#)] [[PubMed](#)]
26. Lin, S.Y.; Harada, M.; Suzuki, Y.; Hatano, H. Comparison of Pyrolysis Products between Coal, Coal/CaO, and Coal/ $\text{Ca}(\text{OH})_2$  Materials. *Energy Fuels* **2003**, *17*, 602–607. [[CrossRef](#)]
27. Müller-Hagedorn, M.; Bockhorn, H.; Krebs, L.; Müller, U. A comparative kinetic study on the pyrolysis of three different wood species. *J. Anal. Appl. Pyrolysis* **2003**, *68–69*, 231–249. [[CrossRef](#)]
28. Patwardhan, P.R.; Satrio, J.A.; Brown, R.C.; Shanks, B.H. Influence of inorganic salts on the primary pyrolysis products of cellulose. *Bioresour. Technol.* **2010**, *101*, 4646–4655. [[CrossRef](#)]
29. Hu, H.; Xie, K.; Chen, T.; Xu, S.; Yang, F.; Li, X.; Li, A.; Yao, H. Performance of calcium-added molten alkali carbonates for high-temperature desulfurization from pyrolysis gases. *Renew. Energy* **2019**, *145*, 2245–2252. [[CrossRef](#)]
30. Sathe, C.; Pang, A.Y.; Li, C.-Z. Effects of Heating Rate and Ion-Exchangeable Cations on the Pyrolysis Yields from a Victorian Brown Coal. *Energy Fuels* **1999**, *13*, 748–755. [[CrossRef](#)]
31. Zeng, K.; Yang, X.; Xie, Y.; Yang, H.; Li, J.; Zhong, D.; Zuo, H.; Nzihou, A.; Zhu, Y.; Chen, H. Molten salt pyrolysis of biomass: The evaluation of molten salt. *Fuel* **2021**, *302*, 121103. [[CrossRef](#)]
32. Yang, Y.; Wang, T.; Zou, C.; Xu, K.; Hu, H.; Gao, L.; Li, X.; Yao, H. Comparing the thermal conversion behavior of bio-wastes in three molten nitrates. *Renew. Energy* **2022**, *196*, 617–624. [[CrossRef](#)]
33. Chen, D.Y.; Gao, A.J.; Cen, K.H.; Zhang, J.; Cao, X.B.; Ma, Z.Q. Investigation of biomass torrefaction based on three major components: Hemicellulose, cellulose, and lignin. *Energy Convers. Manag.* **2018**, *169*, 228–237. [[CrossRef](#)]
34. Zhang, M.; Resende, F.L.; Moutsoglou, A.; Raynie, D.E. Pyrolysis of lignin extracted from prairie cordgrass, aspen, and Kraft lignin by Py-GC/MS and TGA/FTIR. *J. Anal. Appl. Pyrol.* **2012**, *98*, 65–71. [[CrossRef](#)]
35. Tian, X.; Wang, Y.; Zeng, Z.; Dai, L.; Peng, Y.; Jiang, L.; Yang, X.; Yue, L.; Liu, Y.; Ruan, R. Study on the mechanism of co-catalyzed pyrolysis of biomass by potassium and calcium. *Bioresour. Technol.* **2020**, *320*, 124415. [[CrossRef](#)] [[PubMed](#)]
36. Ottah, V.E.; Ezugwu, A.L.; Ezike, T.C.; Chilaka, F.C. Comparative analysis of alkaline-extracted hemicelluloses from Beech, African rose and Agba woods using FTIR and HPLC. *Heliyon* **2022**, *8*, 09714. [[CrossRef](#)] [[PubMed](#)]
37. Chaudhary, R.; Dhepe, P.L. Solid base catalyzed depolymerization of lignin into low molecular weight products. *Green Chem.* **2016**, *19*, 778–788. [[CrossRef](#)]
38. Lee, H.S.; Volesky, B. Interaction of light metals and protons with seaweed biosorbent; Interaction of light metals and protons with seaweed biosorbent. *Water Res* **1997**, *31*, 3082–3088. [[CrossRef](#)]
39. Hattori, M.; Shimaya, Y.; Saito, M. Solubility and Dissolved Cellulose in Aqueous Calcium- and Sodium-Thiocyanate Solution; Solubility and Dissolved Cellulose in Aqueous Calcium- and Sodium-Thiocyanate Solution. *Polym. J.* **1998**, *30*, 49–55. [[CrossRef](#)]
40. Zhao, M.; Cui, X.; Ji, G.; Zhou, H.; Vuppaladadiyam, A.K.; Zhao, X. Alkaline Thermal Treatment of Cellulosic Biomass for  $\text{H}_2$  Production Using Ca-Based Bifunctional Materials. *ACS Sustain. Chem. Eng.* **2018**, *7*, 1202–1209. [[CrossRef](#)]
41. Su, S.; Li, W.; Bai, Z.; Xiang, H.; Bai, J. Effects of ionic catalysis on hydrogen production by the steam gasification of cellulose. *Int. J. Hydrogen Energy* **2010**, *35*, 4459–4465. [[CrossRef](#)]
42. Yu, D.; Jin, G.; Pang, Y.; Chen, Y.; Guo, S.; Shen, S. Gas Characteristics of Pine Sawdust Catalyzed Pyrolysis by Additives. *J. Therm. Sci.* **2020**, *30*, 333–342. [[CrossRef](#)]
43. Wang, W.; Lemaire, R.; Bensakhria, A.; Luart, D. Review on the catalytic effects of alkali and alkaline earth metals (AAEMs) including sodium, potassium, calcium and magnesium on the pyrolysis of lignocellulosic biomass and on the co-pyrolysis of coal with biomass. *J. Anal. Appl. Pyrolysis* **2022**, *163*, 105479. [[CrossRef](#)]
44. Wang, J.; Ma, M.; Bai, Y.; Su, W.; Song, X.; Yu, G. Effect of CaO additive on co-pyrolysis behavior of bituminous coal and cow dung. *Fuel* **2019**, *265*, 116911. [[CrossRef](#)]
45. Feng, D.; Zhao, Y.; Zhang, Y.; Sun, S.; Meng, S.; Guo, Y.; Huang, Y.D. Effects of K and Ca on reforming of model tar compounds with pyrolysis biochars under  $\text{H}_2\text{O}$  or  $\text{CO}_2$ . *Chem. Eng. J.* **2016**, *306*, 422–432. [[CrossRef](#)]
46. Lin, X.; Kong, L.; Cai, H.; Zhang, Q.; Bi, D.; Yi, W. Effects of alkali and alkaline earth metals on the co-pyrolysis of cellulose and high density polyethylene using TGA and Py-GC/MS. *Fuel Process. Technol.* **2019**, *191*, 71–78. [[CrossRef](#)]
47. Fu, P.; Hu, S.; Xiang, J.; Li, P.; Huang, D.; Jiang, L.; Zhang, A.; Zhang, J. FTIR study of pyrolysis products evolving from typical agricultural residues. *J. Anal. Appl. Pyrolysis* **2010**, *88*, 117–123. [[CrossRef](#)]

48. Liu, Q.; Wang, S.; Zheng, Y.; Luo, Z.; Cen, K. Mechanism study of wood lignin pyrolysis by using TG–FTIR analysis. *J. Anal. Appl. Pyrolysis* **2008**, *82*, 170–177. [[CrossRef](#)]
49. Wang, R.; Liu, S.; Li, Q.; Zhang, S.; Wang, L.; An, S. CO<sub>2</sub> capture performance and mechanism of blended amine solvents regulated by N-methylcyclohexylamine. *Energy* **2020**, *215*, 119209. [[CrossRef](#)]
50. Zanganeh, K.E.; Shafeen, A.; Salvador, C. CO<sub>2</sub> Capture and Development of an Advanced Pilot-Scale Cryogenic Separation and Compression Unit. *Energy Procedia* **2009**, *1*, 247–252. [[CrossRef](#)]
51. Chen, W.; Li, K.; Xia, M.; Chen, Y.; Yang, H.; Chen, Z.; Chen, X.; Chen, H. Influence of NH<sub>3</sub> concentration on biomass nitrogen-enriched pyrolysis. *Bioresour. Technol.* **2018**, *263*, 350–357. [[CrossRef](#)] [[PubMed](#)]